

# Fecal Microbial Transplant After Ileocolic Resection Reduces Ileitis but Restores Colitis in IL-10<sup>-/-</sup> Mice

Troy Perry, MD, PhD,\* Juan Jovel, PhD,<sup>†</sup> Jordan Patterson, MSc,<sup>†</sup> Gane Wong, PhD,<sup>†,‡,§</sup> Richard N. Fedorak, MD,<sup>†</sup> Aducio Thiesen, MD, PhD,<sup>||</sup> Bryan Dicken, MD,\* and Karen L. Madsen, PhD<sup>†</sup>

**Background:** Ileocolic resection (ICR) is frequently performed for Crohn's disease; however, disease commonly recurs early in the neoterminal ileum. The aim of this study was to use the IL-10<sup>-/-</sup> mouse to determine the effects of ICR on gut microbiome and immune function and if postoperative fecal microbial transplant (FMT) would improve disease.

**Methods:** ICR was performed in 129S1/SvImJ IL10<sup>-/-</sup> mice followed by FMT using stool from wild-type mice. Sham-transplant mice received their own stool. Stool samples were collected on day 0, day 13 (after ICR), and day 27 (after FMT) for whole metagenome shot-gun sequencing. Mucosal-associated bacteria were quantified with quantitative PCR and visualized by fluorescent in situ hybridization. Tissue cytokines were measured with multiplex arrays and mononuclear phagocyte populations by flow cytometry.

**Results:** Surgery induced microbial functional and taxonomic shifts, decreased diversity, and depleted Bacteroidia and Clostridia. ICR mice had reduced colitis but worse ileitis with bacterial overgrowth, increased translocation, and reduction in tissue macrophages. FMT prevented ileitis but restored colitis and allowed for a bloom of  $\gamma$ -proteobacteria. In the colon, ICR and sham transplant were associated with recruitment of tolerogenic dendritic cells, whereas FMT shifted these immune cell subsets to control profiles along with increasing cytokine levels.

**Conclusions:** This study suggests that surgical-induced immune dysfunction and microbial dysbiosis with impaired clearance may be the underlying cause of the early ulcerations found in the ileum of patients with Crohn's disease after ICR. FMT has an immunostimulatory effect on the postoperative intestine, which was beneficial in preventing ileitis, but detrimental in restoring colonic injury after surgery.

(*Inflamm Bowel Dis* 2015;21:1479–1490)

**Key Words:** colitis, dysbiosis, metagenome, dendritic cells, Crohn's disease

Surgery remains a necessary treatment for most patients with Crohn's disease (CD), with resection of the ileocecal region (ICR) being most common.<sup>1</sup> However, rapid recurrence at the anastomosis commonly occurs, and it is believed that recurrence is due to loss of the ileocecal valve, thereby introducing colonic bacteria into the ileum.<sup>2</sup> Studies in humans and animal models have highlighted the interaction of the gut immune system with its microbial inhabitants as central to CD pathogenesis,<sup>3</sup> but little

work has been performed to study this relationship in postoperative disease. Mononuclear phagocytes (MPs) including macrophages (MΦ) and dendritic cells (DCs) are found in large numbers in the gut lamina propria (LP).<sup>4</sup> Under steady-state conditions, intestinal macrophages clear antigens without evoking inflammatory responses whereas DCs promote tolerance by trafficking antigen to mesenteric lymph nodes and inducing T regulatory cells.<sup>5,6</sup> After surgery, MP subsets undergo significant perturbations because of their recruitment and role in tissue repair and wound healing.<sup>7</sup>

IL-10 gene-deficient (IL-10<sup>-/-</sup>) mice spontaneously develop a patchy chronic inflammation primarily in the ileum, cecum, and colon shortly after weaning.<sup>8,9</sup> The development of colitis in this model is highly dependent on the environment, especially the composition of the gut microbiota, and treatment aimed at modulating the colonic microbiota has shown benefit.<sup>10,11</sup> Recently, a surgical resection model was defined in IL-10<sup>-/-</sup> mice, whereby a severe ileitis developed after ICR, mimicking the human condition.<sup>12</sup> In this study, we further refined this model of ileocecal resection in IL-10<sup>-/-</sup> mice analogous to the procedure commonly performed for ileocecal CD in humans and performed a metagenomic analysis of microbial changes related to surgery. As well, we performed a fecal microbial transplant (FMT) after ICR using stool from healthy wild-type donor animals to attempt to restore microbial diversity and composition.

Supplemental digital content is available for this article. Direct URL citations appear in the printed text and are provided in the HTML and PDF versions of this article on the journal's Web site ([www.ibdjournal.org](http://www.ibdjournal.org)).

Received for publication November 5, 2014; Accepted February 3, 2015.

From the Departments of \*Surgery, <sup>†</sup>Medicine and <sup>‡</sup>Biological Sciences, University of Alberta, Edmonton, AB, Canada; <sup>§</sup>BGI-Shenzhen, Shenzhen, China; and <sup>||</sup>Department of Laboratory Medicine, University of Alberta, Edmonton, AB, Canada.

Supported by Canadian Institutes for Health Research, Alberta Innovates, Alberta IBD Consortium, Canadian Surgical Research Fund, the Edmonton Civic Employees Research Assistance Fund, Alberta Innovates Technology, and Centers of Research Excellence (I-Core).

The authors have no conflicts of interest to disclose.

Reprints: Karen L. Madsen, PhD, Department of Medicine, University of Alberta, 7-142K Katz Building, Edmonton, AB, Canada T6G 2E1 (e-mail: [karen.madsen@ualberta.ca](mailto:karen.madsen@ualberta.ca)).

Copyright © 2015 Crohn's & Colitis Foundation of America, Inc.

DOI 10.1097/MIB.0000000000000383

Published online 19 May 2015.

In that patients undergoing surgery for CD generally have a severe microbial dysbiosis, we hypothesized that performing FMT with healthy donor stool after surgery would have an added benefit in preventing disease recurrence by restoring a healthy microbiome.

## METHODS

### Animal Model

Animal use protocols were approved by the Health Science Animal Care Committee at the University of Alberta. IL-10<sup>-/-</sup>129S1/SvImJ mice (12–13 wk) with established ileocolic inflammation underwent ileocolic resection (ICR) with primary end-to-end anastomosis as previously described.<sup>13</sup> Ileum was transected 2 cm proximal to the ileocecal junction, and the ascending colon divided just distal to cecum (see Fig., Supplemental Digital Content 1, <http://links.lww.com/IBD/A817>). The ileocolic anastomosis was constructed with 8-0 Prolene (Ethicon US, LLC., Cincinnati, OH). The abdominal wall was closed, and animals were maintained on liquid diet for 2 days. Overall survival in the operative groups was 97%. Nonoperative control IL-10<sup>-/-</sup> mice received the liquid diet but did not undergo surgery.

### Fecal Microbial Transplant

Thirteen days after surgery, mice were fasted overnight and given PEG3350 17.9 mEq/L in H<sub>2</sub>O (Golytely; Braintree Laboratories Inc, Braintree, MA). Stools were collected from healthy age-matched wild-type 129S1/SvImJ mice (n = 4) and homogenized in phosphate-buffered saline (PBS) reduced with 0.05% cysteine HCl (Sigma-Aldrich Canada Co, Oakville, Canada) at a ratio of 1 fecal pellet/mL. Previous studies have shown that wild-type mice have significantly different microbial composition compared with IL-10<sup>-/-</sup> mice.<sup>11,14</sup> The fecal slurry was passed through a 100  $\mu$ m cell strainer and 200  $\mu$ L delivered to the FMT group by oral gavage (FMT). A sham transplant group was gavaged with a fecal slurry prepared from their own stools (Sham). The nonoperative control group (CT) was gavaged with PBS 0.05% cysteine HCl. After FMT, mice were placed on chow. On d28, mice were killed and tissues collected (see Fig., Supplemental Digital Content 1, <http://links.lww.com/IBD/A817>).

### Histological Analyses

Perianastomotic sections of ileum and colon were fixed in 10% buffered formalin, embedded in paraffin, cut at 5  $\mu$ m, and stained with hematoxylin/eosin or Masson's trichrome for analysis.<sup>15</sup> A validated histological injury scale scored enterocyte injury, epithelial hyperplasia, LP lymphocytes, LP neutrophils, and peri-intestinal inflammation. Masson's trichrome stains were scored from 0 to 2 for collagen deposition.<sup>15</sup>

### 16S rRNA Quantitative PCR

Genomic DNA was extracted using FastDNA Spin kit (MP Biomedicals) and quantified on a ND-1000 NanoDrop spectrophotometer (Thermo Fisher Scientific, Waltham, MA). Samples were

diluted to 50 ng/mL and then requantified with PicoGreen (Invitrogen, Life Technologies Inc., Burlington, Canada). Quantitative PCR (qPCR) reactions contained 8  $\mu$ L H<sub>2</sub>O, 10  $\mu$ L Fast SYBR Green Master Mix, 1  $\mu$ L 10  $\mu$ M forward and reverse primers, and 2  $\mu$ L target DNA (see Table, Supplemental Digital Content 2, <http://links.lww.com/IBD/A818>). Sequence of PCR conditions was 5 minutes at 50°C, 5 minutes at 95°C (15 sec at 95°C, 1 min at 60°C) (40 cycles), followed by a melting curve step progressing from 60°C to 95°C over 12 minutes. qPCR was performed in MicroAmp 96-well optical plates with the 7900HT instrument. Results were analyzed with SDS 2.3 software. Nonspecific amplification was determined using melting curves and visualizing products on a QIAxcel (Qiagen Inc, Toronto, Canada). Target DNA copy number was determined by comparison with standard curves constructed from purified PCR product obtained using the primers in Table, Supplemental Digital Content 2, <http://links.lww.com/IBD/A818> and quantified using the PicoGreen assay (Invitrogen) to amplify genomic DNA from stool in standard PCR reactions. Gene copy number per nanogram of genomic DNA was determined based on the starting concentration of genomic DNA in each reaction.

### Fluorescent In Situ Hybridization

Tissue sections were deparaffinized in xylene, washed in 100% ethanol, and dried at 50°C. Fluorescent in situ hybridization staining was performed using Cy3-labeled EUB 388 probe, which specifically binds the 16S rRNA gene for the domain bacteria.<sup>16</sup> A nonspecific probe was used for negative controls. DNA probes were diluted to 5 ng/ $\mu$ L in hybridization buffer (0.9 M NaCl, 0.02 M Tris-HCl, 5% formamide, and 0.05% sodium dodecyl sulfate). Hybridization occurred in a humidified chamber at 50°C for 90 minutes. Slides were rinsed in H<sub>2</sub>O and placed in wash buffer (0.636 M NaCl, 0.02 M Tris-HCl, and 0.006% sodium dodecyl sulfate) at 50°C. Slides were rinsed in H<sub>2</sub>O, counterstained with DAPI, and mounted with FluorSave mounting media (Calbiochem; Millipore Canada Ltd., Etobicoke, Canada).

### Characterization of LP Cells

LP cells were isolated by washing intestinal tissues in Hank's balanced salt solution with 5% fetal bovine serum (HBSS/FBS) plus 2 mM EDTA at 37°C for 20 minutes to remove epithelial cells. Tissues were minced and digested in HBSS/FBS plus 1.5 mg/mL collagenase type VIII (Sigma) and 40  $\mu$ g/mL DNase I (Invitrogen) for 20 minutes. MP populations were enriched using CD11b/CD11c microbeads and the LS MACS column following manufacturers protocols (Miltenyi Biotec, San Diego, CA). Cells were stained with the LIVE/DEAD fixable aqua dead cell stain kit (Invitrogen), washed and incubated for 20 minutes with antibody cocktail containing PerCP-conjugated anti-mouse CD45, PE-conjugated anti-mouse CD103, APC-conjugated anti-mouse CD11c, AlexaFluor 700-conjugated anti-mouse I-Ab, eFluor 450-conjugated anti-mouse CD11b, and PE-Cy7-conjugated anti-mouse F4/80 in PBS with 5% fetal bovine serum.<sup>17</sup> Cells were fixed in 2% paraformaldehyde in PBS and analyzed on a BD Biosciences FACS Canto II flow cytometer.

## Tissue Cytokines

Snap frozen perianastomotic colon and ileum were homogenized in PBS containing 0.05% Tween 20 and then centrifuged at 10,000 rpm for 10 minutes. Supernatant was used for measurement of cytokines after correction for dry tissue weight using the Proinflammatory Panel 1 V-PLEX Mouse Kit (MesoScale Discovery, Rockville, MD) as per manufacturer's protocol. Thymic stromal lymphopoietin was measured using an enzyme-linked immunosorbent assay duo set (R&D Systems, Inc., Minneapolis, MN).

## Metagenomic Analysis

DNA was extracted from stools using the FastDNA Spin Kit for feces (MP Biomedicals, Santa Ana, CA). Libraries were constructed using 1 ng of stool DNA and the Nextera XT (Illumina, Inc., San Diego, CA) protocol. The Nextera XT transposome was used to fragment DNA and to incorporate sequencing adapters into the fragments termini, followed by a 12-cycle PCR indexing reaction. Primer dimers and low-molecular-weight PCR products were removed using half a volume of Agencourt AMPure XP paramagnetic beads (Beckman Coulter Canada, Burlington, Canada). Libraries were quantified using the Agilent high-sensitivity DNA kit and sequenced in a MiSeq using a paired-end 300-cycle protocol. Libraries with less than 50,000 reads were eliminated. Sequences were aligned to the NCBI nonredundant nucleotide database (nt) using the LAST algorithm,<sup>18</sup> which implements an adaptive seed approach. LAST was run with default parameters. Metagenomics classification was performed using the Meta Genome Analyzer, MEGAN5,<sup>19</sup> with the following parameters: maxMatches = 100, minScore = 50.0, maxExpected = 0.01, topPercent = 10.0, minSupport = 50, and minComplexity = 0.44. Paired-end analysis was enabled. For inference of the coding capacity of the bacteriome, reads classified as bacteria were mapped to the last version of the KEGG pathway database (June 2011). Principal coordinates analyses of taxonomic or functional data were also performed using MEGAN5 and the KEGG database.

## Statistical Analysis

All data are expressed as the mean  $\pm$  SEM. Statistical analysis was performed using Graphpad Prism version 5.04 and mean values compared for significant differences using Student's one-way analysis of variance with Tukey–Kramer post hoc test. Results from metagenomic analysis were evaluated for significance using the LEfSe tool with *P* values set at 0.05, a linear discriminant analysis cutoff score of 3.0, and all-against-all class comparison.<sup>20</sup>

# RESULTS

## Histological Analyses

The nonoperative control group (CT) had colitis as characterized by enterocyte injury, epithelial hyperplasia, and immune cell infiltration (Fig. 1B). All mice that underwent ICR (sham and FMT) developed fibrosis (data not shown) and ileitis

(Fig. 1A). Those mice that received FMT after ICR had decreased ileitis (*P* < 0.05) as compared with the group that received a sham transplant (sham) (Fig. 1A). This was associated with reductions in enterocyte injury and neutrophil infiltration. Colitis was not improved in the group receiving FMT but was reduced in the sham group as compared with the CT group (Fig. 1B).

## Mucosal-associated Bacteria

To examine if the histological injury patterns were associated with changes in mucosal-associated bacteria, qPCR was used to quantify specific bacteria. The sham group had decreased colonic (Fig. 2B) but increased ileal (Fig. 3B) bacterial loads, which correlated with histological injury. Bacteria were also visualized in the ileal LP of the sham group but not in the FMT or control groups (Fig. 3A). In the colon, the FMT group had increased bacteria in the LP (Fig. 3A). Both ICR groups had reduced colonic *Clostridium* cluster IV and *Bacteroides-Prevotella-Porphyromonas*, whereas sham animals had increased colonic *Lactobacillus-Pediococcus-Leuconostoc* and FMT animals had increased *Enterobacteriaceae* (Fig. 2C). Compositional perturbations in the ileum were less dramatic as *Bacteroides-Prevotella-Porphyromonas* organisms remained dominant across all groups (Fig. 3C); however, *Clostridium* cluster IV was decreased in both ICR groups and *Lactobacillus-Pediococcus-Leuconostoc* was elevated in the sham group.

## Analyses of MPs

MP subsets in the ileal LP were defined as CD45<sup>+</sup>MHC-II<sup>+</sup> cells that were CD11b<sup>-</sup>CD11c<sup>+</sup> (R1), CD11b<sup>+</sup>CD11c<sup>+</sup> (R2), and CD11b<sup>+</sup>CD11c<sup>-</sup> (R3). These subsets were further defined based on expression of the DC marker CD103 and the macrophage (MΦ) marker F4/80.<sup>21</sup> Gating strategy is presented in Figure 4A. After ICR, sham animals had significant perturbations in ileal MP subsets (Fig. 4B). The CD11b<sup>-</sup>CD11c<sup>+</sup> population, which typically consists of CD103<sup>+</sup> DCs, had an increased proportion of CD103<sup>-</sup> cells.<sup>21</sup> The CD11b<sup>+</sup>CD11c<sup>+</sup> population consists of both MΦ and DCs. The sham group had decreased F4/80<sup>+</sup> MΦ and increased F4/80<sup>-</sup> CD103<sup>-</sup> cells. Prior characterization of the CD11b<sup>+</sup>CD11c<sup>-</sup> population defines them as primarily F4/80<sup>+</sup> MΦ.<sup>21</sup> Our data are consistent with this observation; however, the sham group again demonstrated a reduction in this MΦ subset and a reciprocal increase in F4/80<sup>-</sup> cells. MP subsets in the ileum of the FMT group reflected nonoperative controls, consistent with decreased bacterial load and tissue injury. After gating for CD45<sup>+</sup>MHC-II<sup>+</sup> cells, colonic MP subsets were determined by defining DCs as CD11c<sup>+</sup>CD103<sup>+</sup> and MΦ as CD11b<sup>+</sup>F4/80<sup>+</sup> (Fig. 5A, B). FMT led to an increase in CD103<sup>+</sup> DCs in the colon and a shift toward CD11b<sup>+</sup>CD103<sup>+</sup> DCs (Fig. 5A), which are known to accumulate with colitis.<sup>21</sup> Consistent with decreased colonic injury, the sham group had a higher proportion of CD11b<sup>-</sup>CD103<sup>+</sup> DCs, which are primarily defined by their pro-regulatory properties.<sup>6</sup> F4/80<sup>+</sup> MΦ were increased in both ICR groups with a shift to the CD11c<sup>-</sup>F4/80<sup>+</sup> subset in the FMT group (Fig. 5B).



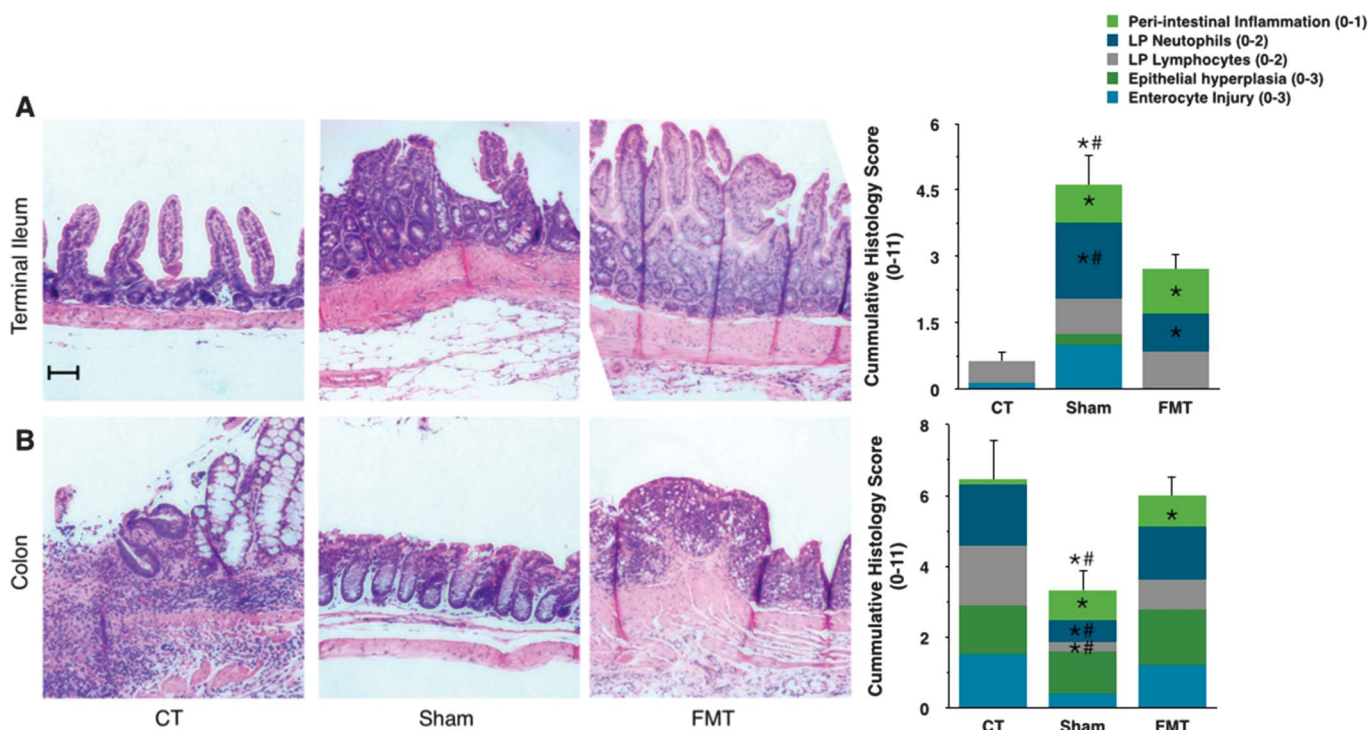


FIGURE 1. Photomicrographs and histological injury scores. Tissue sections of terminal ileum and colon at  $\times 10$  magnification for nonoperative control animals (CT), sham microbial transplant animals (sham), and fecal transplant animals (FMT). Bar graphs represent mean  $\pm$  SEM cumulative injury scores and individual components of the score ( $n = 6$  per group). (A), CT animals had minimal ileal injury. Sham animals had increased histological injury characterized by enterocyte injury, infiltrating neutrophils, and peri-intestinal inflammation. FMT animals had increased neutrophil infiltration and peri-intestinal inflammation compared with CT but had decreased enterocyte injury and neutrophil infiltration relative to sham. (B), In the colon, CT animals had elevated injury scores with enterocyte injury and ulceration, neutrophil and lymphocyte infiltration, and epithelial hyperplasia. Lymphocyte and neutrophil infiltration were reduced in the sham animals relative to both CT and FMT groups. Scale bar represents 100  $\mu\text{m}$ . \* $P \leq 0.05$  relative to CT; # $P \leq 0.05$  relative to other ICR group.

## Tissue Cytokine Levels

All ICR mice had increased ileal levels of interleukin (IL)-1 $\beta$ , IL-5, and interferon gamma, whereas the FMT group had a further increase in tumor necrosis factor alpha (TNF- $\alpha$ ) and CXCL1 (Fig. 4C). The FMT group also showed a reduction in thymic stromal lymphopoietin suggesting alterations in epithelial cell function. The sham group had reduced colonic levels of IL-1 $\beta$ , IL-6, TNF- $\alpha$ , and CXCL1 relative to nonoperative controls. Donor stool transplant in the FMT group restored cytokines to the level of nonoperative controls and led to further increases in TNF- $\alpha$ , interferon gamma, and IL-2.

## Effects on the Gut Microbiome

Whole metagenome sequencing was performed on stools collected before surgery and transplant and at sacrifice for longitudinal analysis on taxonomic and functional genomic shifts associated with ICR and FMT. To determine the attributes of specific microbes that may have conferred a survival benefit after surgery, functional annotation was applied to the metagenomic sequences. Orthologous genes were grouped into broad functional categories and metabolic pathways based on the BRITE hierarchy.

At baseline, microbiota was similar across all groups (see Fig., Supplemental Digital Content 3, <http://links.lww.com/IBD/A819>). Bacteroidetes and Firmicutes represented the major phyla with minor contributions from Proteobacteria and Actinobacteria (see Fig. A, Supplemental Digital Content 3, <http://links.lww.com/IBD/A819>). Substantial microbial diversity was seen at the genus level (see Fig. B and D, Supplemental Digital Content 3, <http://links.lww.com/IBD/A819>).

## Effects of Surgery

After surgery, there was a significant loss of microbial diversity with predominance of Firmicutes and expansion of Proteobacteria (Fig. 6A, B). At the genus level, *Lactobacillus* dominated (Fig. 6B and see Fig., Supplemental Digital Content 4, <http://links.lww.com/IBD/A820>). Clades positively associated with ICR included *Streptococcus*, *Enterococcus*, *Turicibacter*, and *Staphylococcus* (see Fig., Supplemental Digital Content 5, <http://links.lww.com/IBD/A821>). Clades decreased with ICR largely consisted of obligate anaerobic species. Principal coordinates analyses of the Bray-Curtis dissimilarity index revealed differential clustering of ICR and nonoperative CT animals at

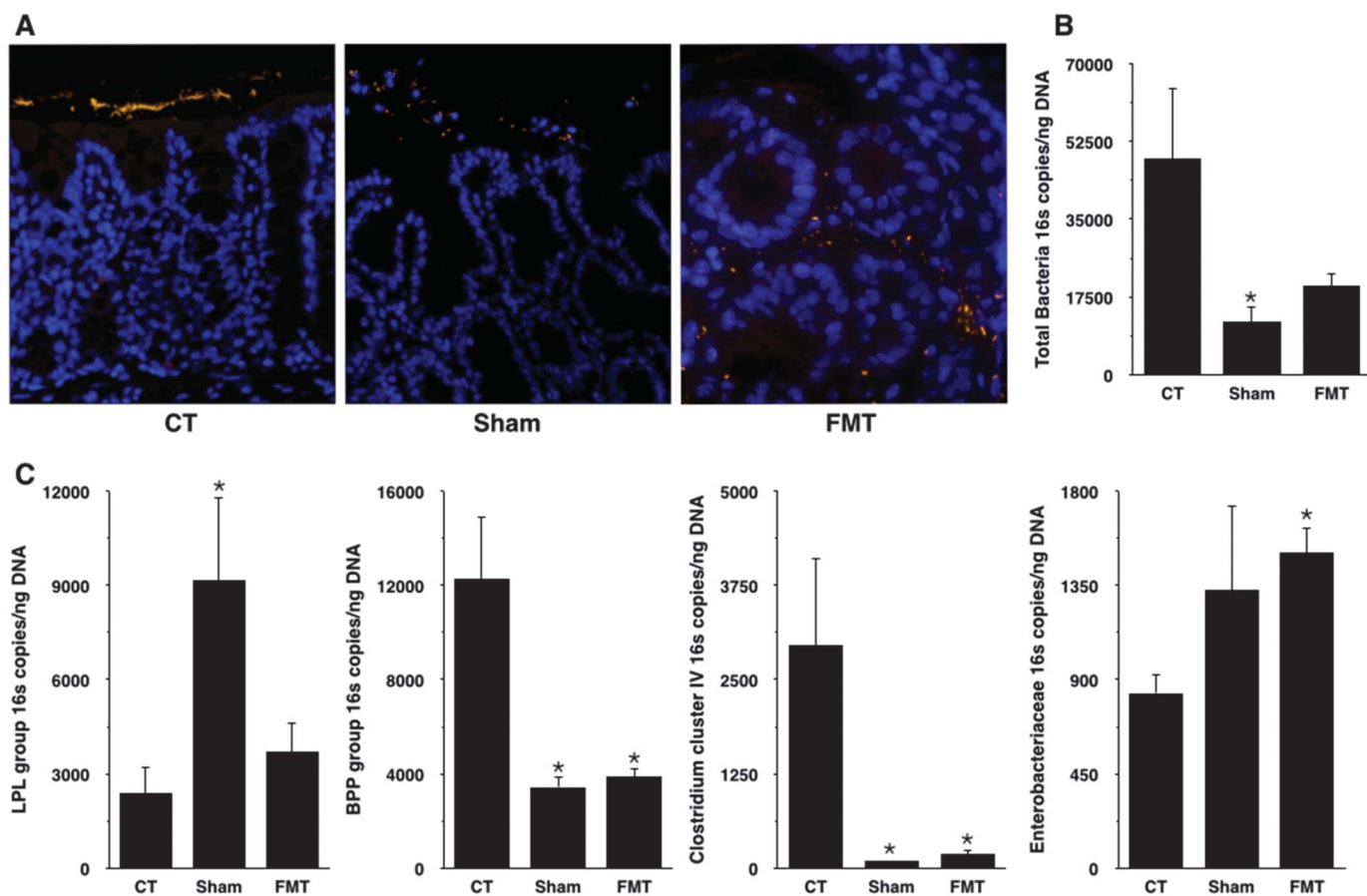


FIGURE 2. Quantification and localization of colonic mucosal-associated bacteria. (A), Photomicrographs of colonic tissues processed by fluorescent in situ hybridization with the EUB 388 probe (orange) and DAPI (blue) at  $\times 40$  magnification. CT and sham groups demonstrate bacteria in the lumen, whereas bacteria were found in the LP of the FMT group. (B), qPCR results for total bacteria showed sham and FMT animals to have decreased colonic bacterial loads. (C), Sham and FMT groups had reduced *Clostridium* cluster IV and *Bacteroides-Prevotella-Porphyromonas* (BPP). Sham animals had increased colonic *Lactobacillus-Pediococcus-Leuconostoc* (LPL). FMT animals had increased *Enterobacteriaceae*. All bar charts represent mean  $\pm$  SEM 16s rRNA gene copy number per nanogram of genomic DNA ( $n = 6$  per group). \* $P \leq 0.05$  relative to CT.

d13 (Fig. 6C). There was an increased gene abundance of the glutathione metabolic pathway and thioredoxin reductase enzymes (Fig. 6F), both of which are important for protection against oxidative damage.<sup>22</sup> There was no change in other enzymes specific to oxidative stress such as catalase, superoxide dismutase, and peroxidase (data not shown). ABC transporters and the phosphotransferase system both demonstrated increased relative abundance at d13, which may be related to bile acid resistance.<sup>23</sup> Significant shifts in the metabolic potential of the metagenome were found suggestive of a highly auxotrophic and resistant population. Carbohydrate and lipid metabolism, membrane transport, and xenobiotic degradation were all increased after ICR (Fig. 6E), but pathways for the biosynthesis of fatty acids, unsaturated fatty acids, and steroid hormones were decreased (see Table, Supplemental Digital Content 6, <http://links.lww.com/IBD/A822>). Moreover, despite increased butyrate metabolism, the final genes for the 2 butyrate synthetic pathways, acetate CoA-transferase, and butyrate kinase were undetectable after ICR (see Fig. A, Supplemental Digital Content

7, <http://links.lww.com/IBD/A823>), suggesting a loss of butyrate production. Loss of biosynthetic capacity in the post-ICR metagenome was also reflected by decreases in amino acid and vitamin metabolic categories (Fig. 6E).

### Effects of FMT

Fourteen days after FMT, rarefaction analysis (Fig. 7D) revealed persistently decreased diversity in both ICR groups despite substantial diversity in the donor stool (Fig. 7B). The sham-transplanted group continued to have increased *Lactobacillus*, *Enterococcus*, *Streptococcus*, and *Staphylococcus* relative to control and FMT groups (Fig. 7A, B). In the FMT group, the only clade elevated was *Klebsiella* (see Fig., Supplemental Digital Content 8, <http://links.lww.com/IBD/A823>), which uniformly expanded in all animals after donor transplantation despite low relative abundance in donor stool (Fig. 6B). Principal coordinates analyses at d27 demonstrated tight clustering of nonoperative CT animals with wider divergence seen in the sham transplant and FMT groups (Fig. 7C). An additional LefSe analysis was performed to compare the effect

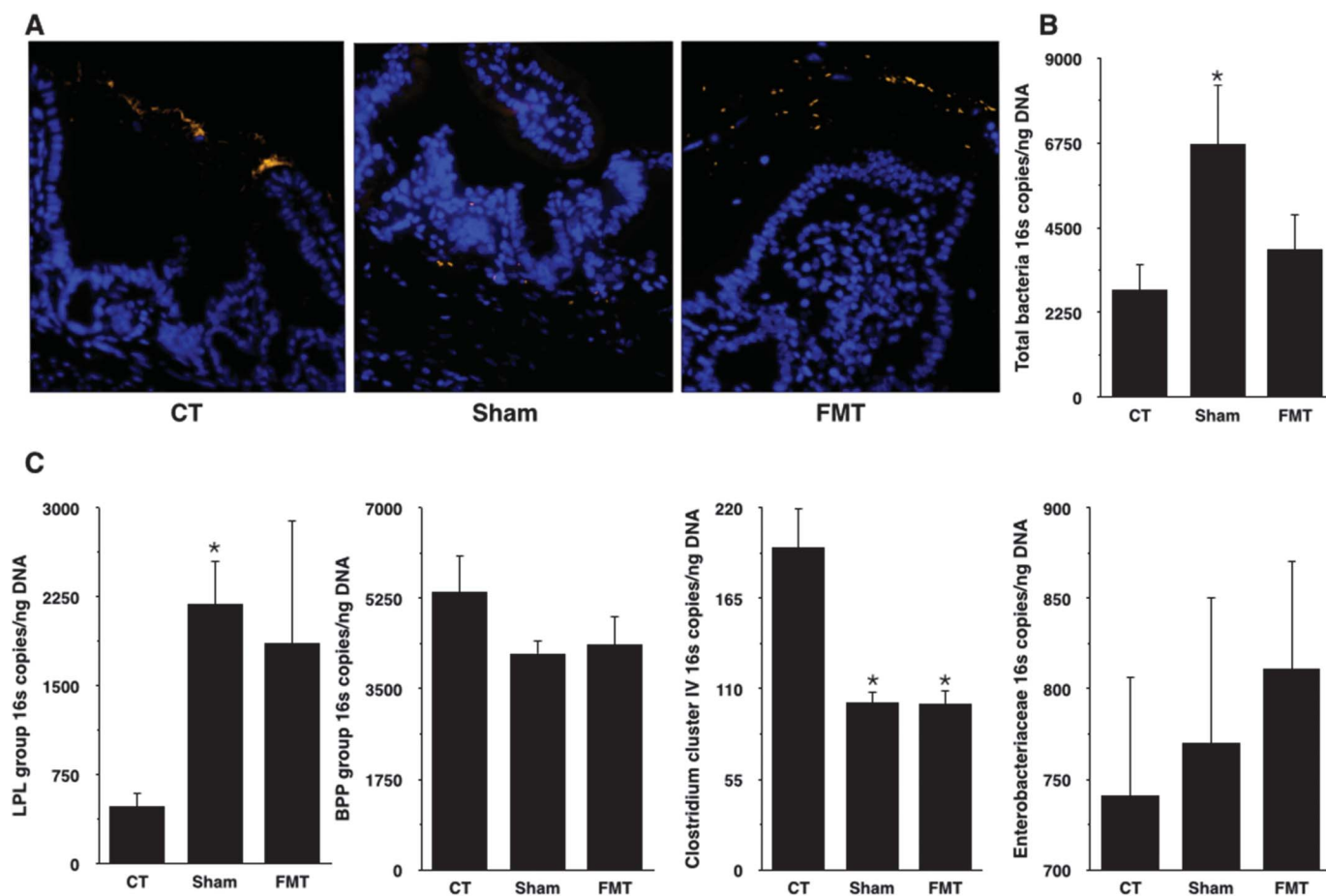


FIGURE 3. Quantification and localization of ileal mucosal-associated bacteria. (A), Photomicrographs of ileal tissues processed by fluorescent in situ hybridization with the EUB 388 probe (orange) and DAPI (blue) at  $\times 40$  magnification. Sham group demonstrated bacteria in the LP. Bacteria were only found in the lumen in CT and FMT groups. (B), qPCR results for total bacteria showed sham animals to have increased ileal bacterial load. (C), Clostridium cluster IV was decreased in sham and FMT, and LPL was elevated in sham. All bar charts represent mean  $\pm$  SEM. 16s rRNA gene copy number per nanogram of genomic DNA ( $n = 6$  per group). BPP, *Bacteroides-Prevotella-Porphyromonas*; LPL, *Lactobacillus-Pediococcus-Leuconostoc*. \* $P \leq 0.05$  relative to CT.

of FMT in the ICR animals alone by only considering sham and FMT groups at d27 (see Fig., Supplemental Digital Content 4, <http://links.lww.com/IBD/A820>). In addition to *Klebsiella*, this analysis revealed increases in *Bacteroides*, *Alistipes*, and *Parabacteroides* in FMT animals. *Klebsiella* and *Bacteroides* accounted for the majority of the relative abundance (Fig. 7B). Metagenomic analysis of the sham group suggested that a simple metagenome with lipid metabolism and membrane transport increased relative to the other groups (Fig. 7E). Several functional pathways were increased, mostly within carbohydrate metabolism (see Table, Supplemental Digital Content 6, <http://links.lww.com/IBD/A822>). In the FMT group, numerous functional perturbations associated with the restoration of colonic injury were seen, including increased carbohydrate metabolism, xenobiotics degradation and metabolism, metabolism of other amino acids, and signal transduction (Fig. 7E). Mice that received FMT showed decreased butanoate metabolism and increased glutathione metabolism, sulfur metabolism, benzoate degradation, and 2 component signaling (Fig. 7F). Additionally, enzymes specific to aerotolerance were increased in FMT animals

(see Fig. B, Supplemental Digital Content 7, <http://links.lww.com/IBD/A823>). Genes for LPS biosynthesis and glycosaminoglycan degradation were elevated in FMT animals and may have contributed to the increased colonic injury (Fig. 7F).

## DISCUSSION

In this study, surgical resection resulted in decreased colonic but increased ileal inflammation. Bacterial overgrowth in the neoterminal ileum and increased bacterial invasion into the LP together with alterations in macrophages and DCs were associated with ileal injury. FMT after surgery failed to restore microbial diversity and allowed expansion of  $\gamma$ -proteobacteria and restoration of colitis. However, FMT improved ileal inflammation, reduced ileal mucosal-associated bacterial loads, and restored MP cell subsets to similar profiles as seen in nonoperative control animals indicative of immune stimulation.

The disparate results between the terminal ileum and the colon may be due to their unique biology. Although the colon has



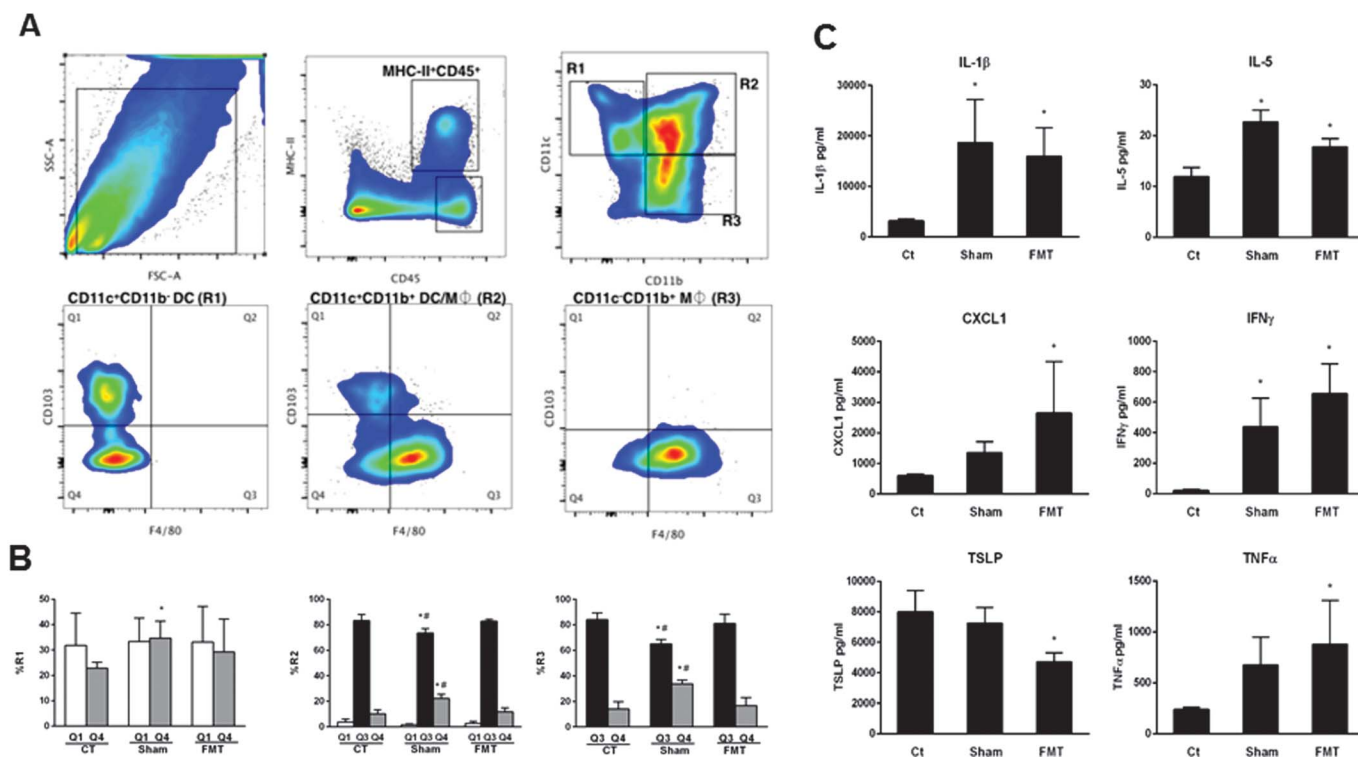


**FIGURE 4.** Characterization of mononuclear phagocyte populations in the ileal LP and tissue cytokines. (A), Fluorescence-activated cell sorting plots demonstrating gating strategy for ileal populations. Cells were positively selected for CD11b/CD11c expression using a magnetic column, then pregated for live cells. (B), Populations R1, R2, and R3 were evaluated for expression of CD103 and F4/80. Bar charts represent mean  $\pm$  SEM proportion of cells expressing F4/80 or CD103 from the 3 subsets. Sham animals had an increased proportion of CD103 cells in the CD11b<sup>+</sup>CD11c<sup>+</sup> population, a decrease in F4/80<sup>+</sup> M $\Phi$ , and an increase in F4/80<sup>+</sup>CD103<sup>+</sup> cells (B). Data are representative of 6 independent experiments. (C), Ileal cytokines (mean  $\pm$  SEM) corrected for tissue dry weight. Sham and FMT ( $n = 7$ ) animals had increased tissue levels of IL-1 $\beta$ , IL-5, and interferon gamma (IFN- $\gamma$ ). FMT animals had increased TNF- $\alpha$  and CXCL1 and decreased thymic stromal lymphopoietin. \* $P \leq 0.05$  relative to CT, # $P \leq 0.05$  relative to other ICR group.

a thick mucus layer, which prevents microbial contact with the epithelium, the ileum is well equipped for microbial sampling and clearance with a high density of gut-associated lymphoid tissues, leukocyte-rich LP, and antimicrobial peptide production from paneth cells. In this study, qPCR demonstrated that ileal mucosal-associated bacteria both increased in numbers and showed compositional changes after surgery. In particular, there was an increase in the aerotolerant *Lactobacilli* group along with a decrease in anaerobic *Clostridium* cluster IV. During surgery, the bowel is exposed to atmospheric oxygen for a period of time, and it follows that microbes able to cope with oxidative stress would have a survival advantage. *Clostridium* cluster IV is a major butyrate producer, and depletion of butyrate-producing bacteria in inflammatory bowel disease microbiota has been shown.<sup>24</sup> Butyrate is a major energy source for enterocytes, and lack of butyrate can lead to energy deprivation, reduced barrier function, and increased bacterial translocation.<sup>25</sup> Overall, the microbiome in CD demonstrates a loss of numerous processes important for gut health including short chain fatty acid, vitamin, and amino acid biosynthesis, along with increased aerotolerance, nutrient import, and toxin secretion, similar to our animal model.<sup>26</sup> Thus,

it could be postulated that a reduction in butyrate production because of a decrease in *Clostridium* cluster IV could have played a role in the microbial and immunological changes observed after surgery.

In the sham group, there were significant shifts in ileal LP MP population. The observed reduction in M $\Phi$  was likely responsible for the increased ileal neutrophils and bacterial invasion, as these cells are essential for clearance of invading gut microbes and also function to phagocytize neutrophils as part of the healing response.<sup>27</sup> Previous studies have reported that the phagocytic function of neutrophils is inhibited as a result of surgery, as is their motility and production of antimicrobial compounds.<sup>28</sup> Macrophage function has also been shown to be impaired after surgery.<sup>29</sup> The uniform increase in cells not expressing CD103 or F4/80 in all 3 CD11b/CD11c subsets is intriguing and may represent a larger relative abundance of immature monocyte populations. Although further characterization is required, it is likely that a proportion of these cells are acting as myeloid-derived suppressor cells.<sup>30</sup> Myeloid-derived suppressor cells, defined by the CD11b and Gr1 markers, are known to have potent immunosuppressive properties. Furthermore, they are known to increase after surgical or

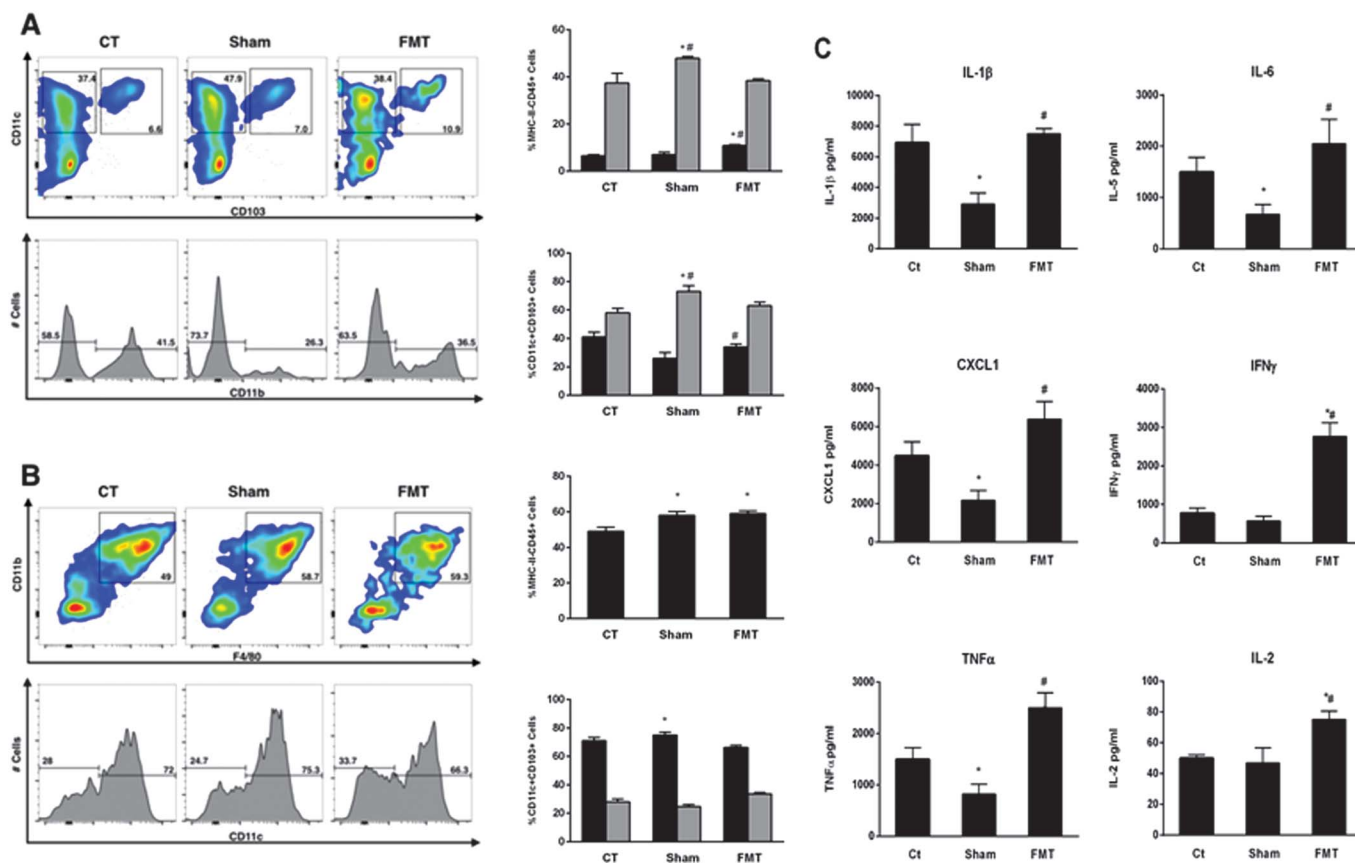


FIGURE 5. Colonic mononuclear phagocyte populations and tissue cytokines. (A), Fluorescence-activated cell sorting plots demonstrate cell populations pregated for live CD45<sup>+</sup>MHC-II<sup>+</sup> cells. Results show mean  $\pm$  SD from 6 independent experiments. (A), Proportion of antigen-presenting cells expressing CD11c<sup>+</sup>CD103<sup>+</sup> or CD11c<sup>+</sup>CD103<sup>-</sup>. CD11c<sup>+</sup>CD103<sup>+</sup> dendritic cells were further classified by CD11b expression. (B), Proportion of antigen-presenting cells expressing CD11b<sup>+</sup>F4/80<sup>+</sup>. This macrophage population was further characterized by CD11c expression. FMT animals had an increase in CD103<sup>+</sup> DCs and a shift toward CD11b<sup>+</sup>CD103<sup>+</sup> DCs. Sham animals had a higher proportion of CD11b<sup>-</sup>CD103<sup>+</sup> DCs. F4/80<sup>+</sup> M $\Phi$  were increased in both ICR groups with a shift to the CD11c<sup>+</sup>F4/80<sup>+</sup> subset in the FMT group. Colonic cytokines (mean  $\pm$  SEM) corrected for dry weight. Sham animals had reduced levels of IL-1 $\beta$ , IL-6, TNF- $\alpha$ , and CXCL1 relative to CT. Donor stool transplant in the FMT group restored cytokines to the level of nonoperative controls and led to further increases in TNF- $\alpha$ , interferon gamma (IFN- $\gamma$ ), and IL-2. \* $P \leq 0.05$  relative to CT. # $P \leq 0.05$  relative to other ICR group.

traumatic stress.<sup>31</sup> FMT restored all MP subsets in the LP to reflect controls. This was associated with a decreased bacterial load, absence of bacteria within the LP, and decreased enterocyte injury and neutrophil infiltration. It is possible that the increased antigenic stimulation from the FMT was responsible for this immune stimulation and restorative effect. Although the cytokine profiles in tissue homogenates reflected a proinflammatory state in both surgery groups, these profiles reflect a combination of epithelial, immune, and fibroblast cells and likely represent a state of low-grade inflammation due to injury and bacterial overgrowth in the sham-transplant mice and immune activation and microbial clearance in the fecal transplant group. Indeed, the increased TNF- $\alpha$  and interferon gamma levels in the fecal transplant group suggest a Th1/M1 response and reversal of the potential immunosuppressive effects.

Concurrently, with the induction of ileitis, surgery also reduced colitis and inflammatory cytokines. The underlying mechanism of this effect likely involves a combination of

surgical-induced immune suppression related to activation of the hypothalamic-pituitary-adrenal axis<sup>28</sup> together with a surgical-induced alteration in gut microbial composition.<sup>32</sup> During healing responses, MP populations will shift toward an alternatively activated immunosuppressive phenotype.<sup>7</sup> We demonstrated that CD11c<sup>+</sup>CD103<sup>+</sup>CD11b<sup>-</sup> DCs were increased in the colonic LP; these cells have well-established regulatory activities.<sup>6</sup> It is likely that oxidative stress related to surgery resulted in the selection of *Lactobacillus*, *Enterococcus*, and *Streptococcus* that provided a low-complexity community in the colon that contributed to the suppression of inflammation. Expansion of *Lactobacillus* species has previously been reported after intestinal surgery.<sup>32,33</sup> Studies evaluating *Lactobacillus* spp as probiotics have demonstrated their anti-inflammatory effects, ability to stimulate mucin production, and bacteriocin production,<sup>34</sup> and some of these may have contributed to the reduction in colitis. Relative to controls, functional characteristics with known associations to inflammation in the



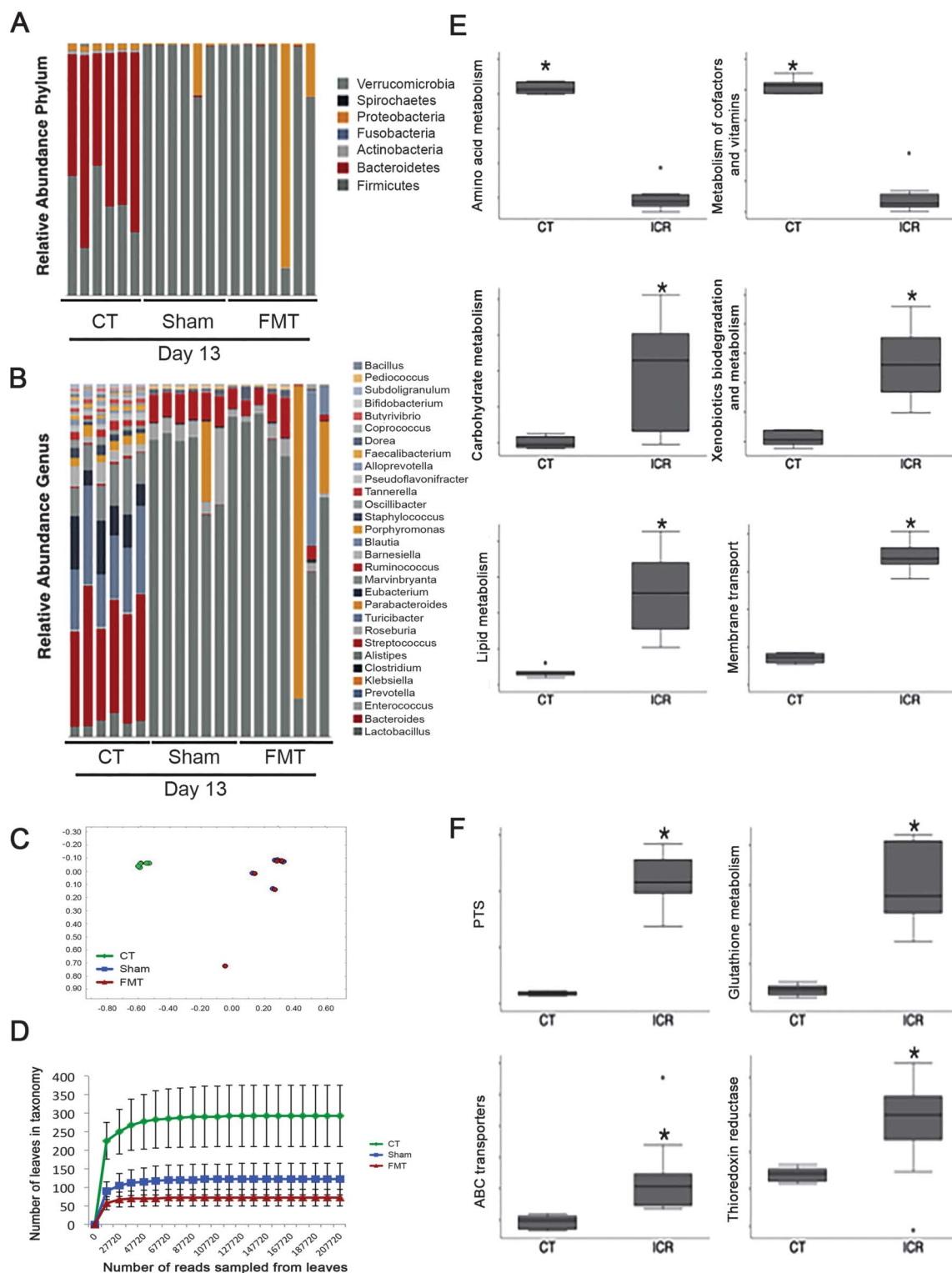


FIGURE 6. Metagenomic analysis after surgery. Relative abundance of major phyla (A) and genera (B) at d13 after surgery. Each bar represents relative abundance from 1 individual mouse. (C), Principal coordinates analyses plot of the Bray-Curtis index ( $n = 6$  per group). (D), Rarefaction analysis at d13. Curves represent mean  $\pm$  SD for each experimental group ( $n = 6$  per group). ICR caused loss of diversity with taxonomic and functional shifts in the gut microbiome. (E), Median relative abundance of functional categories in controls ( $n = 6$ ) versus ICR ( $n = 14$ ). (F), Median relative abundance of functional pathways and genes. Significant associations were determined using the LEfSe tool with a linear discriminant analysis cutoff score of 3.0 (\*). PTS, phosphotransferase system.

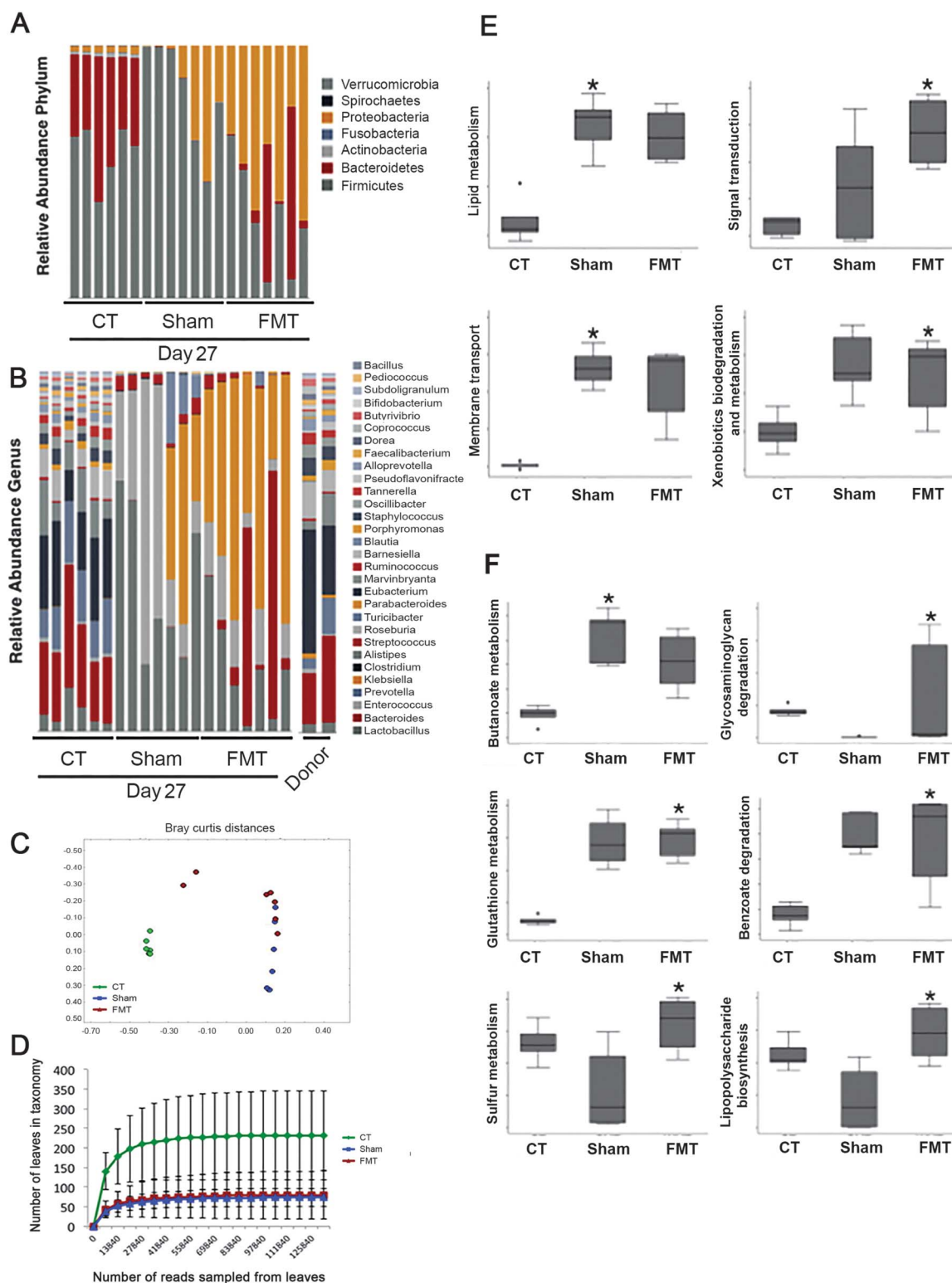


FIGURE 7. Metagenomic analysis of effects of FMT after surgery. Relative abundance of major phyla (A) and genera (B) at day 27. Each bar represents relative abundance from 1 individual mouse. (C), Principal coordinates analyses plot of the Bray-Curtis index ( $n = 6$  CT group,  $n = 7$  sham and FMT). (D), Rarefaction analysis at day 27. Curves represent mean  $\pm$  SD for each experimental group. FMT did not restore diversity but did cause taxonomic and functional shifts. (E), Median relative abundance of functional categories. (F), Median relative abundance of functional pathways. Significant associations were determined using the LEfSe tool with a linear discriminant analysis cutoff score of 3.0 (\*).

gut metagenome such as flagella assembly were also reduced.<sup>35</sup> However, interestingly, the decrease in colitis occurred even with the loss of butyrate producers from the *Clostridium* cluster IV group and butyrate producing enzymes.

In our study, colitis was increased after FMT. This was associated with an expansion of both *Klebsiella* and *Bacteroides*, which are known to cause colitis in IL10<sup>-/-</sup> mice because of the mucolytic capacity of these bacteria.<sup>36,37</sup> Results from the functional metagenome analysis support this, as demonstrated by increased capacity for glycosphingolipid degradation in the fecal transplant group. Increased capacity to survive oxidative stress may form an alternative positive feedback loop selecting for pathobionts like *Klebsiella* with colitogenic properties. However, the immune response is likely also involved in the colonic injury. An antigenic load provided by the fecal transplant may have shifted the immune response from immunosuppressive to a recruitment of proinflammatory monocyte subsets including CD11c<sup>+</sup>CD11b<sup>+</sup>CD103<sup>+</sup> DCs, thus restoring inflammatory cytokine signaling.<sup>38</sup> The increased inflammatory cytokines in combination with mucolytic bacteria could have the additive effect of allowing for increased bacterial translocation, which we observed in the colon of FMT mice.

The increased bacterial load in the neoterminal ileum seen in our model is similar to that seen in humans after resection.<sup>39</sup> Results from this study may help explain the efficacy of early postoperative antibiotics in preventing postoperative recurrence, as the ileal segment is unable to appropriately deal with invading microbes in the postoperative period.<sup>40</sup> Furthermore, the induction of a gut microbiome with low complexity because of oxidative stress could facilitate the overgrowth of pathogens and/or pathobionts, which may eventually colonize the vulnerable neoterminal ileum, providing an explanation for the occurrence of invasive *Escherichia coli* in postoperative CD lesions.<sup>41</sup>

In conclusion, we propose that surgery causes a loss of microbial diversity and induction of aerotolerant organisms that together with impaired microbial clearance because of immunosuppression results in bacterial overgrowth and increased translocation in the neoterminal ileum. In this scenario, ileocecal resection could be likened to a forest fire, where an ecological niche is burnt to the ground necessitating the formation of a new gut ecosystem. The nature of this restoration may be open to manipulation to prevent the recurrence of gut inflammation with directed immunomodulation and/or stimulation, antibiotics, probiotics, and prebiotics.

## ACKNOWLEDGMENTS

Author contributions: J. Jovel, J. Patterson, and A. Thiesen were involved with data analysis and revision of the manuscript. T. Perry was involved with study concept and design, acquisition of data, analysis of data, and drafting of manuscript. G. Wong was involved with study supervision and critical revision of the manuscript. R. N. Fedorak, B. Dicken, and K. L. Madsen were involved in study concept and design, interpretation of data, and critical revision of the manuscript.

## REFERENCES

1. Frolkis AD, Dykeman J, Negron ME, et al. Risk of surgery for inflammatory bowel diseases has decreased over time: a systematic review and meta-analysis of population-based studies. *Gastroenterology*. 2013;145:996–1006.
2. Rutgeerts P. Strategies in the prevention of post-operative recurrence in Crohn's disease. *Best Pract Res Clin Gastroenterol*. 2003;17:63–73.
3. Abraham C, Medzhitov R. Interactions between the host innate immune system and microbes in inflammatory bowel disease. *Gastroenterology*. 2011;140:1729–1737.
4. Varol C, Zigmund E, Jung S. Securing the immune tightrope: mononuclear phagocytes in the intestinal lamina propria. *Nat Rev Immunol*. 2010;10:415–426.
5. Smythies LE, Sellers M, Clements RH, et al. Human intestinal macrophages display profound inflammatory anergy despite avid phagocytic and bacteriocidal activity. *J Clin Invest*. 2005;115:66–75.
6. Scott CL, Aumeunier AM, Mowat AM. Intestinal CD103<sup>+</sup> dendritic cells: master regulators of tolerance? *Trends Immunol*. 2011;32:412–419.
7. Novak ML, Koh TJ. Phenotypic transitions of macrophages orchestrate tissue repair. *Am J Pathol*. 2013;183:1352–1363.
8. Kühn R, Löhler J, Rennick D, et al. Interleukin-10-deficient mice develop chronic enterocolitis. *Cell*. 1993;75:263–274.
9. Doyle J, Jewell L, Madsen K, et al. Intestinal histopathology in interleukin 10 gene knock out mice resembles Crohn's disease. In: Sutherland L, ed. *Trends in Inflammatory Bowel Disease Therapy*. Higham, MA: Kluwer Academic; 1997:281–284.
10. Berg DJ, Davidson N, Kuhn R, et al. Enterocolitis and colon cancer in interleukin-10-deficient mice are associated with aberrant cytokine production and CD4<sup>+</sup> TH1-like responses. *J Clin Invest*. 1996;98:1010–1020.
11. Madsen KL, Doyle JS, Tavernini MM, et al. Antibiotic therapy attenuates colitis in interleukin 10 gene-deficient mice. *Gastroenterology*. 2000;118:1094–1105.
12. Rigby RJ, Hunt MR, Scull BP, et al. A new animal model of postsurgical bowel inflammation and fibrosis: the effect of commensal microflora. *Gut*. 2009;58:1104–1112.
13. Perry T, Borowiec A, Dicken B, et al. Murine ileocolic bowel resection with primary anastomosis. *J Vis Exp*. 2014.
14. Maharshak N, Packey CD, Ellermann M, et al. Altered enteric microbiota ecology in interleukin 10-deficient mice during development and progression of intestinal inflammation. *Gut Microbes*. 2013;4:316–324.
15. Borowiec AM, Sydnor BC, Doyle J, et al. Small bowel fibrosis and systemic inflammatory response after ileocolonic anastomosis in IL-10 null mice. *J Surg Res*. 2012;178:147–154.
16. Mylonaki M, Rayment NB, Rampton DS, et al. Molecular characterization of rectal mucosa-associated bacterial flora in inflammatory bowel disease. *Inflamm Bowel Dis*. 2005;11:481–487.
17. Geem D, Medina-Contreras O, Kim W, et al. Isolation and characterization of dendritic cells and macrophages from the mouse intestine. *J Vis Exp*. 2012:e4040.
18. Kielbasa SM, Wan R, Sato K, et al. Adaptive seeds tame genomic sequence comparison. *Genome Res*. 2011;21:487–493.
19. Huson DH, Mitra S. Introduction to the analysis of environmental sequences: metagenomics with MEGAN. *Methods Mol Biol*. 2012;856:415–429.
20. Segata N, Izard J, Waldron L, et al. Metagenomic biomarker discovery and explanation. *Genome Biol*. 2011;12:R60.
21. Denning TL, Norris BA, Medina-Contreras O, et al. Functional specializations of intestinal dendritic cell and macrophage subsets that control Th17 and regulatory T cell responses are dependent on the T cell/APC ratio, source of mouse strain, and regional localization. *J Immunol*. 2011;187:733–747.
22. Arner ES, Holmgren A. Physiological functions of thioredoxin and thioredoxin reductase. *Eur J Biochem*. 2000;267:6102–6109.
23. Fang F, Li Y, Bumann M, et al. Allelic variation of bile salt hydrolase genes in *Lactobacillus salivarius* does not determine bile resistance levels. *J Bacteriol*. 2009;191:5743–5757.
24. Morgan XC, Tickle TL, Sokol H, et al. Dysfunction of the intestinal microbiome in inflammatory bowel disease and treatment. *Genome Biol*. 2012;13:R79.
25. Ploger S, Stumpff F, Penner GB, et al. Microbial butyrate and its role for barrier function in the gastrointestinal tract. *Ann N Y Acad Sci*. 2012;1258:52–59.



26. Kostic AD, Xavier RJ, Gevers D. The microbiome in inflammatory bowel disease: current status and the future ahead. *Gastroenterology*. 2014;146:1489–1499.
27. Lech M, Grobmayr R, Weidenbusch M, et al. Tissues use resident dendritic cells and macrophages to maintain homeostasis and to regain homeostasis upon tissue injury: the immunoregulatory role of changing tissue environments. *Mediators Inflamm*. 2012;2012:951390.
28. Hogan BV, Peter MB, Shenoy HG, et al. Surgery induced immunosuppression. *Surgeon*. 2011;9:38–43.
29. Wu GJ, Tai YT, Chen TL, et al. Propofol specifically inhibits mitochondrial membrane potential but not complex I NADH dehydrogenase activity, thus reducing cellular ATP biosynthesis and migration of macrophages. *Ann N Y Acad Sci*. 2005;1042:168–176.
30. Ostanin DV, Bhattacharya D. Myeloid-derived suppressor cells in the inflammatory bowel diseases. *Inflamm Bowel Dis*. 2013;19:2468–2477.
31. Zhu X, Herrera G, Ochoa JB. Immunosuppression and infection after major surgery: a nutritional deficiency. *Crit Care Clin*. 2010;26:491–500, ix.
32. Hartman AL, Lough DM, Barupal DK, et al. Human gut microbiome adopts an alternative state following small bowel transplantation. *Proc Natl Acad Sci U S A*. 2009;106:17187–17192.
33. Joly F, Mayeur C, Bruneau A, et al. Drastic changes in fecal and mucosa-associated microbiota in adult patients with short bowel syndrome. *Biochimie*. 2010;92:753–761.
34. Stephani J, Radulovic K, Niess JH. Gut microbiota, probiotics and inflammatory bowel disease. *Arch Immunol Ther Exp (Warsz)*. 2011;59:161–177.
35. Rooks MG, Veiga P, Wardwell-Scott LH, et al. Gut microbiome composition and function in experimental colitis during active disease and treatment-induced remission. *ISME J*. 2014;8:1403–1417.
36. Hogenauer C, Langner C, Beubler E, et al. *Klebsiella oxytoca* as a causative organism of antibiotic-associated hemorrhagic colitis. *N Engl J Med*. 2006;355:2418–2426.
37. Bloom SM, Bijanki VN, Nava GM, et al. Commensal *Bacteroides* species induce colitis in host-genotype-specific fashion in a mouse model of inflammatory bowel disease. *Cell Host Microbe*. 2011;9:390–403.
38. Persson EK, Scott CL, Mowat AM, et al. Dendritic cell subsets in the intestinal lamina propria: ontogeny and function. *Eur J Immunol*. 2013;43:3098–3107.
39. Neut C, Bulois P, Desreumaux P, et al. Changes in the bacterial flora of the neoterminal ileum after ileocolonic resection for Crohn's disease. *Am J Gastroenterol*. 2002;97:939–946.
40. Rutgeerts P, Van Assche G, Vermeire S, et al. Ornidazole for prophylaxis of postoperative Crohn's disease recurrence: a randomized, double-blind, placebo-controlled trial. *Gastroenterology*. 2005;128:856–861.
41. Darfeuille-Michaud A, Boudeau J, Bulois P, et al. High prevalence of adherent-invasive *Escherichia coli* associated with ileal mucosa in Crohn's disease. *Gastroenterology*. 2004;127:412–421.